Proposal for the Super-NEMO design study

R. Saakyan, J.Thomas
University College London
S.Söldner-Rembold, A. Pilaftsis
Manchester University

June 23, 2005

1 Executive Summary

The physics goal of Super-NEMO is to search for neutrinoless double beta decay as evidence for Majorana neutrino masses down to the level below 0.05eV, the region pointed to by the oscillation experiments' discovery of neutrino mass.

Super-NEMO is a next generation double beta decay experiment which is under consideration by an international collaboration comprising French, UK, Russian, US, Czech and Japanese collaborators. It is a completely new collaboration which has recently formed with a mixture of new institutes and those which were already involved in the building of previous NEMO experiments. The proposed design elements build on the experience gained over the last 18 years through the NEMO series of experiments. The UK groups are positioning themselves to make a very substantial contribution to this next experiment with serious consideration being given to the Boulby mine as the location. This proposal outlines the steps necessary to finalise the design of a Super-NEMO module, of which Super-NEMO will comprise some 10 or so, and to demonstrate the suitability (or not) of the Boulby mine as the location.

The UK group has been pivotal in bringing the Super-NEMO collaboration to the point of submitting proposals: it is due to our insistence that we are now at this stage. In recognition of the important role the UK is intending to take, the Design Study phase of this project has been essentially split into two parts with the UK leading one (The Tracker) and the French leading the other(The Calorimeter). One of the prerequisites for submitting the proposal was the demonstration of 10% energy resolution for the calorimeter over that demonstrated for NEMO-III. Some of this work was carried out in the UK with funding from the PPRP and the results are attached as an appendix. A resolution of 7-8% was regularly achieved with the correct choice of geometry and materials.

Contents

2 Introduction

Almost three years ago, the UCL group joined the NEMO-III collaboration, and since joining, has been involved with the data analysis of the neutrinoless double beta decay search, background measurements, hardware testing and calibration issues. At about the same time, the UCL authors submitted an SoI in the Super-NEMO experiment to Science Committee. In addition, the UCL group were awarded funds from the PPRP to pursue scintillator R&D whose goal would be to achieve a high resolution electron energy measurement for Super-NEMO. This goal has been achieved and the results from this study are given in Section 18. The Manchester group joined the Super-NEMO collaboration in 2004 and has contributed to a full simulation of the Super-NEMO tracker and has performed a sensitivity and optimization study for the full detector. This proposal builds on the previous investment in this experimental programme and outlines a two year design study programme for optimization of the Super-NEMO modular geometry, calorimeter and tracking parameters. The issue here is to design a detector, knowing the technical building blocks, which is large enough to contain 100 kg of isotopic target while maintaining the background conditions needed to measure the very small signal expected. There are two major goals of this proposal:

- Production of a full technical design of the Super-NEMO module
- Identification of the optimal location for Super-NEMO and the optimal layout of the modules if they are location specific

3 Double Beta Decay

One of the most exciting results of the last decade has been the growing evidence that neutrinos are massive. In the Standard Model neutrinos have only left handed chiral components and therefore must have exactly zero mass. All the fundamental charged fermions are Dirac fermions.

There are presently two neutrino measurements which have started to revolutionise the thinking behind neutrinos: Super Kamiokande and more recently, SNO, which have both shown discrepancies from theoretical predictions while studying atmospheric neutrinos (SK) and solar neutrinos (SK,SNO). The results can be explained by invoking neutrino oscillations as the mechanism for the discrepency which in turn implies that neutrinos have a non-zero mass. The significance of this fact, of course, cannot be overstated but the critical factor which will always elude neutrino oscillation experiments is the positive identification of the fundamental type of the neutrino. All the fermions in the Standard Model are Dirac particles by nature, where the antiparticle is the charge congugate of the particle and has equal but opposite quantum numbers. Neutrinos, however, have an extra possibility due to their neutral charge. It is not forbidden by the gauge symmetries of the Standard Model to add singlet right-haded neutrinos for each left-handed neutrino generation, with heavy Majorana masses of order the GUT scale [9] or some other fundamental sclae of the theory that might be derived from strings[10]. In this case a technically natural solution can be obtained for the smallness of the observed light neutrino masses with respect to the other particles in the SM. Most importantly, the light neutrinos are Majorana particles, which means that neutrinos are their own anti-particles. As shown in Figure1, a salient consequence of the Majorana nature of the neutrinos is that they violate the lepton number by two units, thereby giving rise to neutrinosless double beta decay ($0\nu\beta\beta$)

To search for $0\nu\beta\beta$ decay events as illustrated in Figure 1, experiments must utilize certain nuclei in which this decay is not forbidden energetically. Table 1 lists the double beta decay isotopes and their Q-value, the energy difference between the parent and the daughter nuclei. Figure 2 shows the sum of the energies of the two emitted electrons in the case of $0\nu\beta\beta$ and $2\nu\beta\beta$ as well as the case of the emission of a Majoron particle. Clearly, the $0\nu\beta\beta$ has a very distinct signature and a clear factor when choosing the isotope of study is to ensure that this Q value is as high as possible to discriminate it from natural radioativity which has a maximum energy of about 2.6 MeV.

Table 1: Double beta decay transitions and their $Q_{\beta\beta}$ value

Transition	$Q_{\beta\beta}$(keV)	Abundance%
^{146}Nd→^{146}Sm	56 ±5	17
^{98}Mo→^{98}Ru	112 ±7	24
^{80}Se→^{80}Kr	130 ±9	50
^{122}Sn→^{122}Te	364 ±4	4.6
^{204}Hg→^{204}Pb	416 ±2	7
^{192}Os→^{192}Pt	417 ±4	41
^{186}W→^{186}Os	490 ±2	29
^{114}Cd→^{114}Sn	534 ±4	29
^{170}Er→^{170}Yd	654 ±2	15
^{134}Xe→^{134}Ba	847 ±10	10
^{232}Th→^{232}U	858 ±6	100
^{128}Te→^{128}Xe	868 ±4	32
^{46}Ca→^{46}Ti	987 ±4	-
^{70}Zn→^{70}Ge	1001 ±3	0.6
^{198}Pt→^{198}Hg	1048 ±4	7
^{176}Yb→^{176}Hf	1079 ±3	13
^{238}U→^{238}Pu	1145 ±2	99
^{94}Zr→^{94}Mo	1145 ±2	17
^{154}Sm→^{154}Gd	1252 ±2	23
^{86}Kr→^{86}Sr	1256 ±5	17
^{104}Ru→^{104}Pd	1299 ±4	19
^{142}Ce→^{142}Nd	1418 ±3	11
^{160}Gd→^{160}Dy	1729 ±1	22
^{148}Nd→^{148}Sm	1928 ±2	6
^{110}Pd→^{110}Cd	2013 ±19	12
^{76}Ge→^{76}Se	2040 ±1	8
^{124}Sn→^{124}Te	2288 ±2	6
^{136}Xe→^{136}Ba	2479 ±8	9
^{130}Te→^{130}Xe	2533 ±4	34
^{116}Cd→^{116}Sn	2802 ±4	7
^{82}Se→^{82}Kr	2995 ±6	9
^{100}Mo→^{100}Ru	3034 ±6	10
^{96}Zr→^{96}Mo	3350 ±3	3
^{150}Nd→^{150}Sm	3667 ±2	6
^{48}Ca→^{48}Ti	4271 ±4	0.2

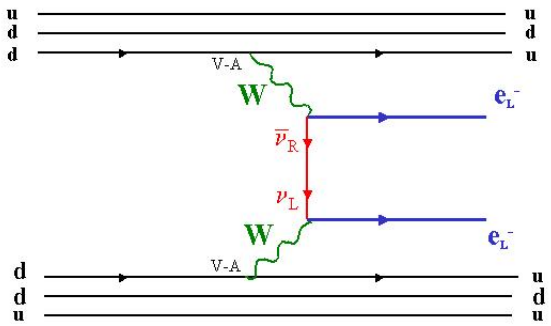

Figure 1: Feynman Diagram depicting neutrinoless double beta decay

Several experiments of this type have published results [2] and plans are underway for a new generation of such experiments to be taking data sometime towards 2008/2010 [3]. The renewed interest in these experiments is due primarily to the results from the Super Kamiokande experiment which has narrowed down the atmospheric neutrino oscillation parameter space, under the assumption that the effects they see are due to $\nu_\mu \rightarrow \nu_\tau$ oscillations. Remembering that oscillations are described by the two parameters $\sin^2 2\theta$ (≈ 1, the strength of the coupling between the two species of neutrino), and Δm^2 , (the difference in the mass squared between the two mass eigenstates) with the very conservative assumption that if Δm^2 $\approx$ 3-10x$10^{-3} eV^2$, and that one of the neutrinos has vanishing mass, it can be deduced that the remaining neutrino must have a mass of at least 0.05eV. This is in the range where the neutrinoless double beta decay experiments will start to be sensitive over the next 5-10 years. How the mass of a single neutrino translates into a Majorana average mass depends on some of the parameters in the neutrino mixing matrix which couple the electron flavour neutrino to the three neutrino mass eigenstates. How the rate of $0\nu\beta\beta$ depends on the mass of the neutrino depends on the nuclear matrix element, which is presently known for some nuclei to within a factor of three, although recent work suggests there might be some room for improvement [4], andon the phase space factor favoring decays with high Q value. Nevertheless, this uncertainty in no way interferes with the ability of the experiment to positively identify neutrinoless double beta decay events, if they occur at a rate which is high enough to be observed above background. Such events have a distinctive signature, where the energy of the two electrons emitted equals the difference in mass between the intial and final isotope. The point where the nuclear matrix element would come in this case would be in the translation of the result to an actual measurement of a mass.

In a three-neutrino mixing framework the weak eigenstate neutrinos ν_e, ν_μ, ν_τ can be expressed as superpositions of 3 neutrino mass eigenstates ν_1, ν_2, ν_3. In particular, electron neutrinos are then superpositions,

$$\nu_e = \sum_i^3 U_{ei} \nu_i$$

where U_{ei} is the neutrino mixing matrix and its elements will be measured by the neutrino oscillation experiments. The halflife of a nucleus due to the $0\nu\beta\beta$ decay is usually expressed as follows:

$$\left[T_{1/2}^{0\nu}\right]^{-1} = G^{0\nu\beta\beta} \left|M^{0\nu}\right|^2 < m_\nu >^2$$

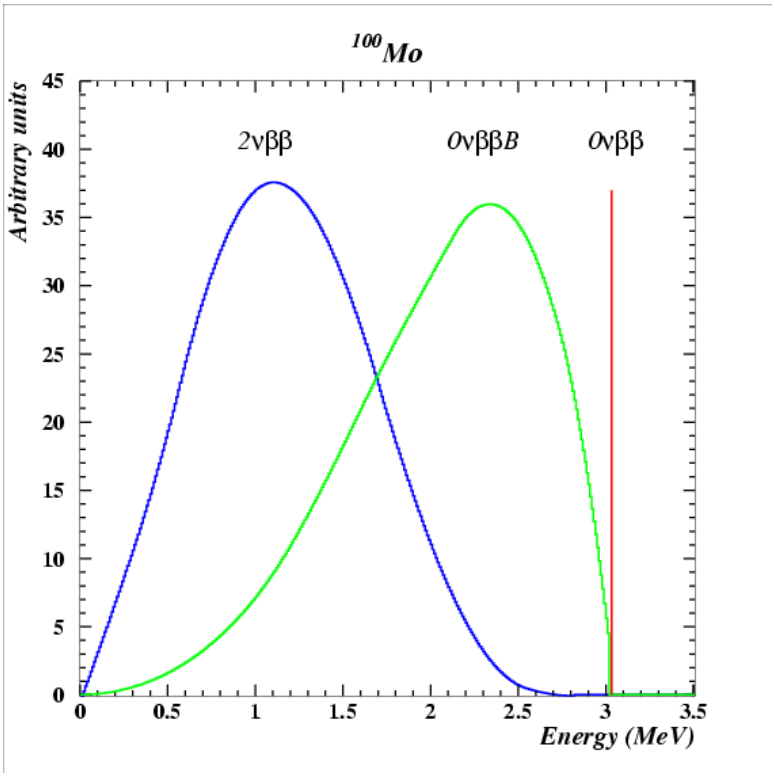

Figure 2: Calculated spectra for ^{100}Mo double beta decay with and without neutrinos

where

where $G^{0\nu}$ and $M^{0\nu\beta\beta}$ are the phase-space factor and the nuclear matrix element, respectively. The quantity $\langle m \rangle$ is the so-called electron Majorana-neutrino mass and describes the electroweak physics of lepton number violation. It can be written down in the following three equivalent forms:

$$\langle m \rangle \;=\; \sum_{i=1}^{3} U_{ei}^{2}\, m_{\nu_i} \;=\; \sum_{i=1}^{3} |U_{ei}|^{2}\, e^{\alpha_i}\, m_{\nu_i} \;=\; m_{ee}\;,$$

where m_{ee} is the $\{11\}$ entry of the 3×3 light-neutrino mass matrix. Moreover, $\langle m \rangle$ depends on the lepton-number-violating Majorana phases α_i which are irrelevant for the lepton-number-conserving neutrino oscillation experiments. Up to theoretical hadronic uncertainties, it is exactly this quantity which is measured by $0\nu\beta\beta$ decay experiments.

Experiments of $0\nu\beta\beta$ decays will be able to address an important key question related to the light neutrino mass spectrum. Since neutrino oscillation experiments only measure squared mass differences, there is an ambiguity in the mass hierarchy. As is illustrated in Figure 3, there are two squared mass differences, $\Delta m^2_{\rm sol}$ and $\Delta m^2_{\rm atm}$: one from the solar neutrino experiments (associated with $\nu_1 \to \nu_2$) and one from the atmospheric experiments (associated with $\nu_2 \to \nu_3$). At present, it is not clear whether ν_3 is heavier or lighter than ν_1 and ν_2. However, as can be seen from Figure 4, the electron Majorana-neutrino mass $\langle m \rangle = m_{ee}$ will exhibit different dependences on the lightest neutrino mass for the proposed normal and inverted hierarchical light neutrino spectra. Thus, observation of a $0\nu\beta\beta$-decay signal would rule out the normal hierarchy scenario.

The new generation of $0\nu\beta\beta$ decay experiments may also offer further insight into the possible nature of new physics beyond the Standard Model. As mentioned above, these experiments may be able to probe the hypothesis of a Majoron-induced $0\nu\beta\beta$ decay [11]. They can put limits on certain fundamental parameters of theories, such as R-parity-violating supersymmetric models [12] and theories with large extra dimensions [13]. They can even test fundamental laws of nature, such as the equivalence principle and Lorentz violation [14].

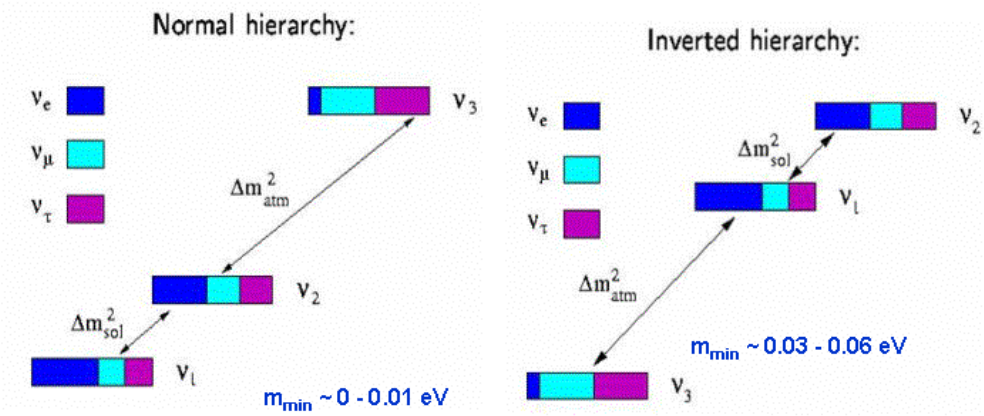

Figure 3: Figure illustrating the ambiguity from the oscillation experiments of the mass hierarchy.

Finally, their synergetic role with other experiments measuring lepton flavour/number violation, e.g. $\mu \rightarrow e\gamma$ or $\mu \rightarrow e$ conversion in nuclei, may provide the fundamental link for the origin of the baryon asymmetry in our Universe [15].

4 The Challenge

Searching for $0\nu\beta\beta$ is difficult. The signal being searched for is so rare and the sources of background so numerous, that the detector design and shielding are particularly challenging. All objects around us have a level of Uranium and Thorium of about 1 part in 10^{6-7} whereas the components of any double beta decay detector must have these impurities at the 1 part in 10^{11-12} in order to keep the background at a manageable level.

From the natural decay chains of ^{238}U and ^{232}Th, only ^{214}Bi and ^{208}Tl are β-decay isotopes with Q_β greater than 3 MeV (with respective Q_β values of 3.270 and 4.992 MeV, and respective half-lives of 19.9 and 3.05 minutes). Thus, ^{214}Bi and ^{208}Tl produce γ-rays and electrons that are energetic enough to simulate $\beta\beta0\nu$ events at 3 MeV. The most energetic γ-rays have energy of 2.615 MeV and come from ^{208}Tl with a branching ratio is 36%

Radon ^{222}Rn ($T_{1/2}$ = 3.824 days) and thoron ^{220}Rn ($T_{1/2}$ = 55.6 s) are α-decay isotopes, which have ^{214}Bi and ^{208}Tl daughter isotopes respectively. Coming mainly from rocks and present in the air, these are very diffusion prone rare gases which can enter the detector. Subsequent α-decay of these gases gives ^{218}Po and ^{216}Po respectively, which can contaminate the interior of the detector.

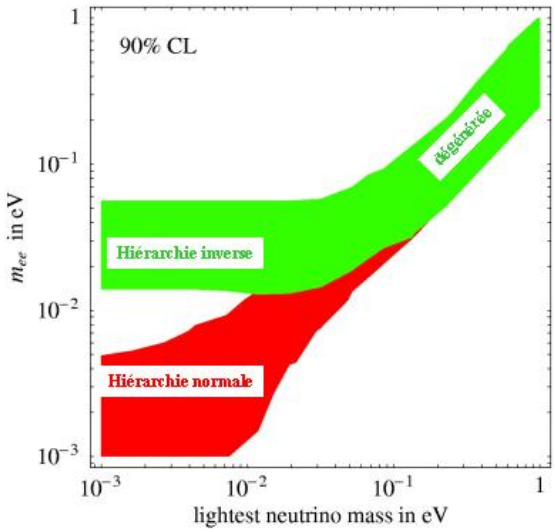

Figure 4: Figure showing the electron neutrino majorana mass reach for the different hierarchies as a function of the lightest neutrino mass

5 Experimental Approaches

There are two distinct experimental approaches in the search for $0\nu\beta\beta$: one is where the $\beta\beta$ source is itself part of the detector such as in Germanium detectors or TeO_2 bolometers. The other is when the source is not part of the detector and a multi-purpose detector suite is arranged around it. The first type typically has very good energy resolution but the disadvantage of weak background discrimination. The second type has worse energy resolution but the advantage of particle identification and event topology recognition. A new approach, which is a hybrid of these two detector types can be seen with the Xenon TPC which combines characteristics from both types of detector but it remains to be seen whether such a detector is superior to the other types.

6 Super-NEMO

Seventeen years of development led to the NEMO-III detector which is one of only two double beta decay experiments presently taking data. In this experiment, the decays from the isotope foils are studied using a suite of standard particle physics detectors, comprising a calorimeter for energy measurement, a tracking detector for electron identification and fast timing for background rejection. The UCL group now have a working knowledge of the analysis and problems of this detector: in particular, the radon level inside the underground lab in Frejus(LSM) has proved higher than originally expected, and technology is now in place to address this. There is also a severe shortage of space at LSM and the Boulby mine potentially provides a perfect environment for this type of experiment because it is a potash mine and there is less ^{238}U ,^{232}Th and therefore radon contamination than in LSM. However, such low levels are difficult to verify without the aid of a very sensitive experiment to measure it. The energy resolution of NEMO-III has proved to be less than optimal for an upgrade to 100kg of DBD isotope (NEMO-III has 10kg of isotope) and a short programme

of R&D has been successfully carried out to address this shortcoming.

6.1 Conceptual Design

The idea for Super-NEMO is to follow the tried and tested technology of the previous NEMO experiments. In abstract, the detector will consist of a tracking volume to measure the paths of the charged particles, a scintillator calorimeter system which will measure the energy of the charged particles and gammas and probably a magnetic field to help in the discrimination between electrons and positrons. The double beta decay isotopes will be in the form of thin foils which will be located inside the tracking volume. The mass of the isotope is expected to be in the region of 100-200kg which corresponds to a reach in Majorana neutrino mass of 0.02-0.07 eV, the range representing the uncertainty in the nuclear matrix element calculations and the final choice of isotope mass.

The R&D described in this proposal is needed to optimize the Super-NEMO design by extrapolating the current technology to an experiment which is one order of magnitude larger than its predecessor.

Unless explicitly states otherwise, we will use a sensitivity for Super-NEMO normalised to 500kg x yr exposure and the most commonly used nuclear matrix element calculation [8]. This will correspond to a sensitivity to the Majorana neutrino mass of 0.04eV.

The fact that the electrons from DBD are very low energy necessitates keeping all energy losses to a minimum. For the tracking detector this probably means Helium gas, which in turn points to Geiger operation of the wires in order to produce a large enough signal to be processed. The source foils should be made as thinly as possible although there are competing effects which ameliorate this particular dependence.

All the materials used in the construction of the detector must be of very high purity and furthermore must be measured to be such. The expertise for producing low background plastic scintillator exists with collaborators in Russia irrespective of the final scintillator material chosen.

6.2 Calorimeter Resolution

The sensitivity of any $0\nu\beta\beta$ experiment depends strongly on the energy resolution of the detector. Provided that the only background is that coming from the high energy $2\nu\beta\beta$ tail, the fraction of the 2ν background events falling in to the 0ν window for a generic *source* = *detector* experiment is proportional to $(\sigma/E)^6$. For a *source* $\neq$ *detector* experiment, like Super-NEMO, the dependence is not that straightforward since the final resolution function is a convolution of the energy resolution of the scintillator detector and the electron energy loss fluctuations in the source foil (Figure 5).

The dependence is therefore a function of the foil thickness. In order to find out how sensitivity is affected by the final energy resolution we have carried out a simplified Monte Carlo simulation of the Super-NEMO detector. This included the simulation of $0\nu\beta\beta$ and $2\nu\beta\beta$ events from a ^{82}Se foil with the following assumptions

- ^{82}Se foils 30 and 60 mg/cm^2 thick.
- Geiger tracking detector with an efficiency for a single track of 0.9 (as measured in NEMO-III).
- ^{214}Bi and ^{208}Tl contamination $\sim 1\mu$Bq/kg or less.
- Alpha-particle detection efficiency (^{214}Bi background reduction) 0.5
- Variable energy window for the $0\nu\beta\beta$ signal with the lowest limit 2.7 MeV and the highest 3.3 MeV

Figure 6 shows the results of these simulations for 500kg$\times$yr data (5 years data taking with 100kg of isotope) 30 mg/cm^2 foil and scintillator energy resolution (FWHM) 15% at 1 MeV (current average resoulution of

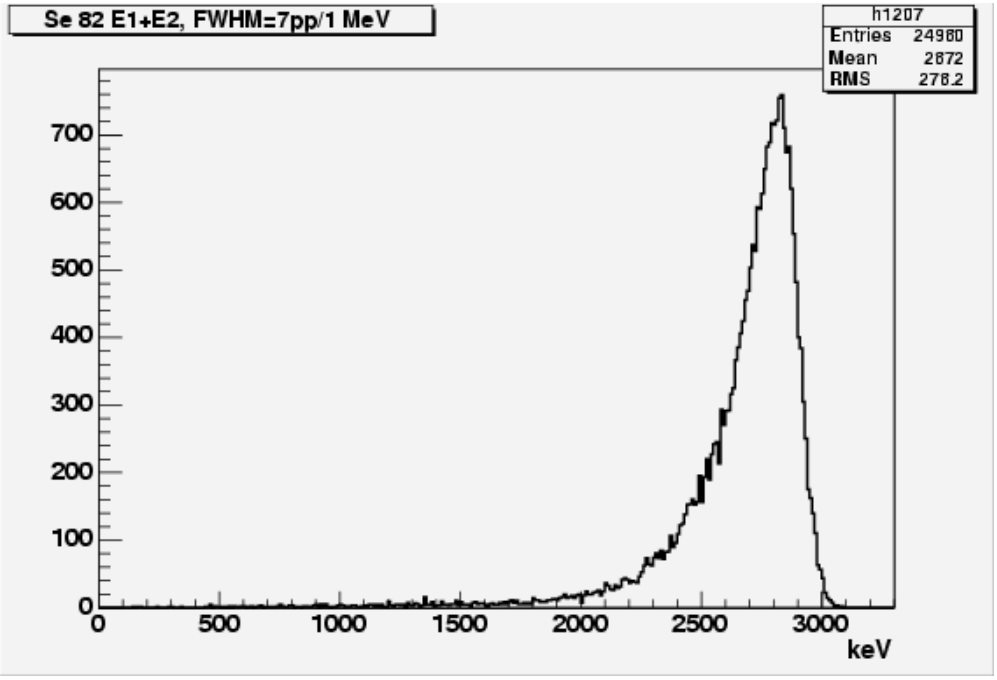

Figure 5: Energy spectrum of $0\nu\beta\beta$ decay simulated with a 30 mg/cm^2 ^{82}Se foil and 7% (FWHM) energy resolution at 1 MeV .

NEMO-3) and 7% at 1 MeV. A very significant benefit in the signal/background ratio in the latter case is evident.

A number of different scintillator energy resolutions have been simulated and their effect on the experimental sensitivity to the effective Majorana neutrino compared. This is summarised in Figure 7 for two source foil thicknesses: 30 and 60 mg/cm^2. Again, 500kg×yr of data have been compared.

One can see from this plot that it is important to reach a calorimeter resolution of 8% or better in order to have a sensitivity to $< m_\nu >$ at the level of 40-50 meV.

Doubling the data sample will reduce this limit to 30-40meV. This has been demonstrated in several scintillators and the PPARC supported work on this subject is reported in Section 18. The key is to make the scintillator thinner than the 20cm block thickness used in NEMO-III such that it will still contain electrons but so that the light is not attenuated too much while exiting the scintillator block. Various approaches have been studied to optimize the light output.

6.3 Possible Detector Layouts

There are a number of possibile detector layouts which are being considered. There is a very important interdependence between the layout, the environment and choice of underground laboratory which affects the type and level of natural background and the aspect ratio of the underground space. For example, the layout depicted in Figure 8 shows the detectors immersed in water for shielding from external neutron and gamma radioactivity. This layout needs a certain ceiling height to enable the detectors to be lowered into the water and raised out of it for maintainence. Another possibility uses the idea of scintillator bar rather than blocks for the calorimeter. This has the advantage that it can be laid down like a "swiss roll" abd the outer modules shield the inner modules and the inner modules shield one side of the outer modules. Such a layout could reduce the number of PMTs by a factor of 4 and make the detector much more compact, thus reducing both the cost and the background.

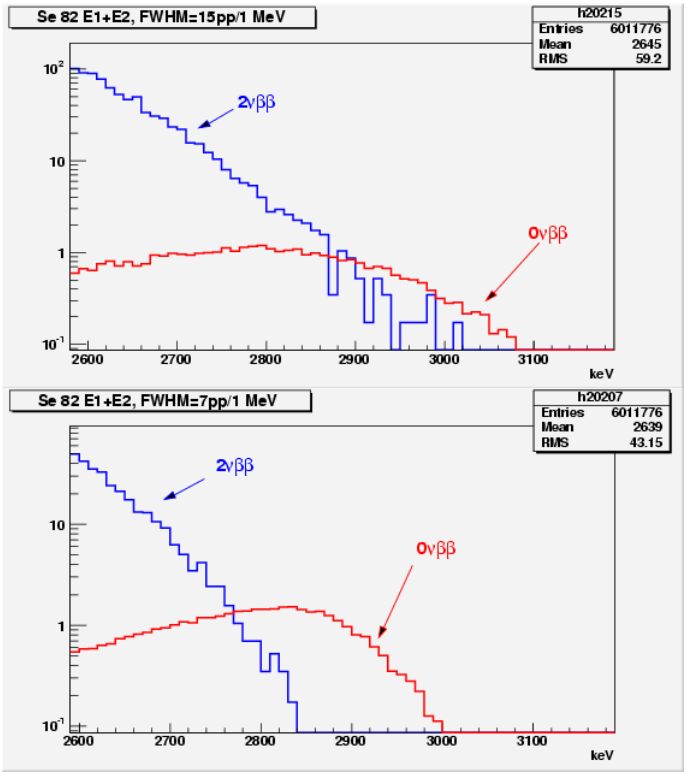

Figure 6: $2\nu\beta\beta$ and $0\nu\beta\beta$ spectra simulated with a 30 mg/cm^2 foil and scintillator energy resolution (FWHM) 15% at 1 MeV (top) and 7% at 1 MeV (bottom) for 500Kgy of data.

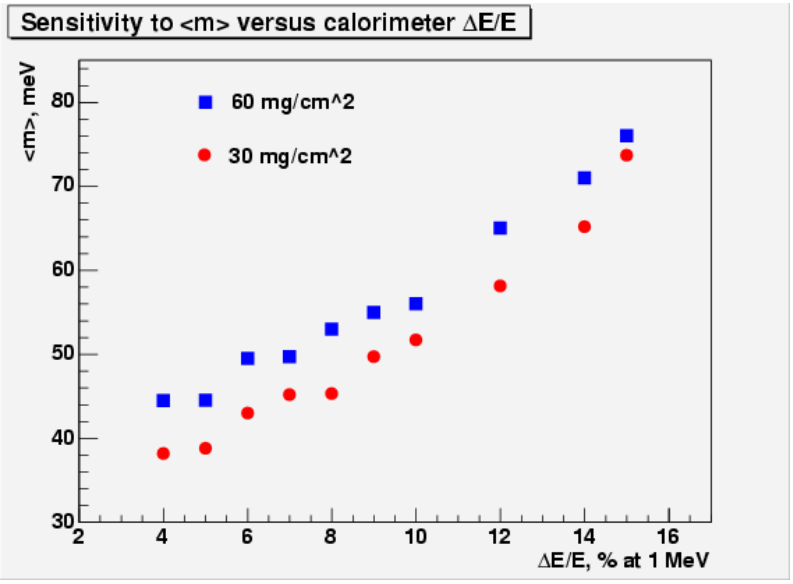

Figure 7: Super-NEMO sensitivity to the effective Majorana mass after 500 kg×yr exposure as a function of the calorimeter energy resolution for 30 and 60 mg/cm^2 ^{82}Se foils using the NME from reference [8]

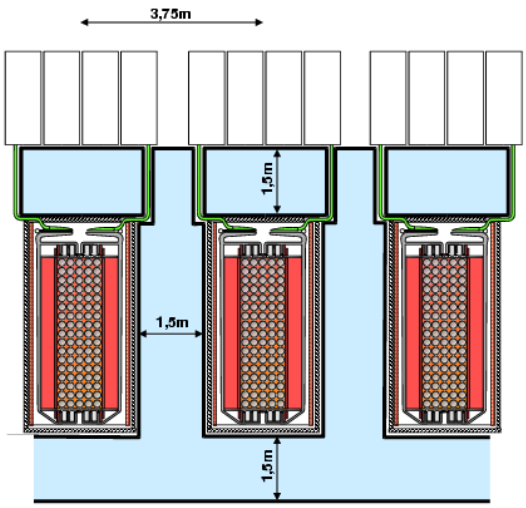

Figure 8: One possible layout for the Super-NEMO detector where the sub-modules are immersed in water for neutron shielding.

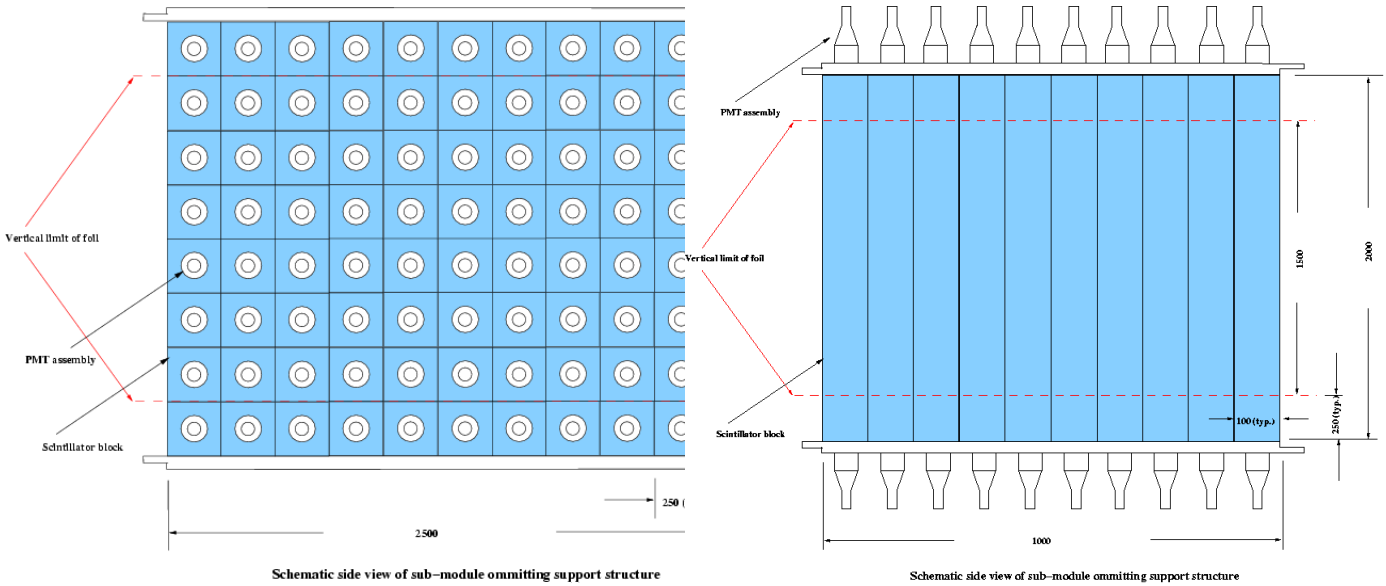

Figure 9: Scintillator bar layout for Super-NEMO

7 Status of other Double Beta Decay Experiments

There are presently a number of projects (15-20) in various stages of planning worldwide which are all attempting to reach the region os 0.03-0.05eV in Majorana neutrino mass. The most advanced designs are EXO and Majorana in the US, CUORE, GERDA and Super-NEMO in Europe. (CUORE is the only one to be fully approved presently). The eventual reach of these next generation detectors are all in the same ballpark as Super-NEMO. The quoted level of Majorana mass reach depends heavily on which calculation for the Nuclear Matrix Element is used for the particular isotope. If SuperNEMO were to start construction after this two year Design Study period, it is possible that this collaboration would be first to reach the desired goal, although CUORE would be the major competition. Most of the experiments require a five year exposure time to reach their required sensitivity. However, even if Super-NEMO is not the first to start taking data, any observation in a calorimeter type experiment where only the energy is measured and not the event topology would have to be confirmed in a SuperNEMO type experiment. In fact, the Heidelberg group has recently announced a discovery of Majorana mass with the best fit value of 0.4eV in a Germanium detector [2]. This is very controversial, but if the real value of ¡m$_{ee}$¿ is indeed close to this value, NEMO-III has a good chance to see the effect in the next 5 years.

8 Milestones and Goals

The goals of this proposal are twofold:

- Production of a full technical design of the Super-NEMO module
- Identification of the optimal location for Super-NEMO and the optimal layout of the modules if they are location specific

On the way to achieving these goals, there are several milestones which need to be reached.

- Optimisation of the number, thickness and composition of Geiger wires in the tracker : Aug 05
- Optimisation of the thickness and composition of the scintillator for the calorimeter and design of the gamma catcher if necessary: Sep 05
- Tracker small prototype: Jan 06
- Prototype of wiring robot: Apr 06
- Electronics design: Jun 06

9 The Super-NEMO Work Breakdown Structure

This programme of work represents an estimate of the work needed to produce a full technical design for the Super-NEMO detector and has been put together in collaboration with the French groups. It should be noted that the schedule reproduced in the gant chart will now be delayed by six months due to slippage in the approval schedule.

The Work Breakdown Structure (WBS) whose main strands are shown in Figure 10 is described in detail below and summarized in the gant chart 12 at the end.

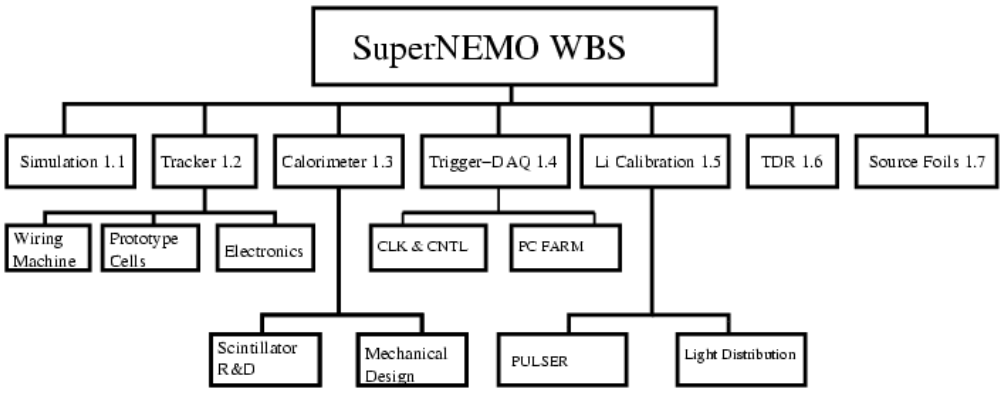

Figure 10: Schematic Representation of the WBS

9.1 Simulation : R.Saakyan/F.Mauger(Caen)

This program simulates the basic geometry and material of the detector, and will use the most up-to-date program version, GEANT-4. This program will eventually be the full-scale simulation of the final Super-NEMO detector.

Input

Work has already started in Manchester on a GEANT simulation of low energy electrons and gammas using GEANT-3 to be used for optimising the geometry for the new, modular, Super-NEMO design. Other inputs are obviously the resolution and geometry from the scintillator and tracker R&D and existing data from NEMO-III.

Output

The full simulation programme including the optimum layout for the very large SUper-NEMO detector.

Milestones

- Optimisation of the number, thickness and composition of Geiger wires in the tracker : Aug 05

Justification of Manpower

The simulation will be performed as part of the calorimeter and tracker design studies by the RA posts with support from graduate students in Manchester and UCL. The workwill be supported and supervised by Saakyan and Söldner-Rembold.

Goal

Identification of the optimal location for Super-NEMO and the optimal layout of the modules if they are location specific.

9.1.1 Active Source

An active foil design is under consideration which consists of two thinner foils (15 mg/cm^2 instead of 50 mg/cm^2) with an active tracking volume in between. The idea is that thinner foils would increase the alpha tagging efficiency. This layout needs to be simulated prior to the prototyping and testing.

9.1.2 Source Thickness

The ultimate energy resolution which can be achieved depends on several parameters, one of which is the source thickness. This is because the electrons lose energy in the source foil as they exit, so the thicker the foil, the worse the energy resolution. This needs to be simulated and its impact on the other design issues studied.

9.1.3 Magnetic Field Simulations

The design of Super-NEMO can in principle be made simpler if there is no need for a magnetic field. Furthermore, the detection efficiency for electrons is increased with no field. Again, data from NEMO-III can answer the question of how important the magnetic field is for background rejection and for electron identification, but detailed simulations are necessary to understand this effect in the context of a particular detector configuration since the need for a magnetic field may depend on the granularity of the scintillator detector, the foil thickness, the need for external gamma tagging to name a few.

9.1.4 Number and Location of Wires

The major source of energy loss for the electrons is scattering from the Geiger wires. Optimisation of the number of wire layers and their layout is one very important task of the simulation. Input from NEMO-III data can be used to verify the importance of the number of wire layers in the track finding and track fitting process. The length of the tracking volume is determined by the timing resolution of the scintillators. The wire planes are not evenly spaced and the location of the wire planes also must take into account additional space constraints due to the scintillators used for photon veto and electron reconstruction at the sides of the chambers. Detailed simulation must determine the optimal spacing and location of the wire planes.

9.1.5 Overall Layout

The overall layout of the Super-NEMO modules is dependent on a number of issues, including the calorimeter design, and the area, and volume, of the underground facility. This task is somewhat iterative, in that it needs input from many other tasks before it is concluded. A planar geometry has significant advantages for building a large detector compared to a cylindrical geometry as used in NEMO-III. A planar geometry is simpler to build and a larger volume of almost arbitrary length can be constructed by joining individual modules. It would also allow for multi-stage production where parts of the detector can be operated before the full-size detector is available. An example of a planar geometry lay-out is shown in Fig. 11. A modular design must also allow for separate construction of the tracking detector, the calorimeter and the source.

The total efficiency including the geometrical acceptance must be increased by about 50% compared to NEMO-III. This optimisation requires detailed simulations of the geometry and design of the tracking chambers and simulations using a GEANT-3 simulation of the detector have been carried in the last months.

9.1.6 Study of Possible Site

Some of the results of the optimisation process may have a bearing on which possible sites are ideal. For example, the possibility of shielding using water is very attractive for some geometrical layouts. This type of issue can be very site specific and some time needs to be assigned to understanding which design issues have an impact on the possible site.

9.2 Tracker : S. Söldner-Rembold and J.Thomas

Input:

Results from the simulation of the wire thickness and layout and previous experience from NEMO-III construction.

Output:

Full design of the tracker for TDR. 100 cell prototype to demonstrate feasability of full-scale Super-NEMO module. Working prototype and design for a full-scale wiring robot. Readout electronics design.

Justification of Manpower

The R&D which will lead to the 100 cell prototype will mainly be performed at Manchester by Söldner-Rembold using the expertise of Ray Thomson and Steve Snow. A significant part of the Manchester RA position is needed to complete this work. It needs technical support from Andrew Elvin and Julian Freestone. The electronics will be designed by a combination of Scott Kolya and an MSSL electrical engineer. The design of the wiring machine will be overseen by Thomas together with an MSSL engineer and technician. Brian Payne (ex RAL) has agreed to act in a consulting role to ensure a transfer of expertise to the younger personel at MSSL.

Milestones

- Optimisation of the number, thickness and composition of Geiger wires in the tracker : Aug 05
- Tracker small prototype: Jan 06
- Prototype of wiring robot: Apr 06
- Electronics design: Jun 06

The tracking detector is a central part of the Super-NEMO design. It is essential for online triggering and offline identification of $\beta\beta$ events and it is needed to suppress internal and external backgrounds.

The current NEMO-III tracking detector is a cylindrical volume separated into 20 sectors with 309 drift cells each adding up to 6180 open octagonal drift cells. The drift cells operate in Geiger mode, they are 270 cm long and have a diameter of 3 cm. They consist of eight cathode wires at 0 V and one anode wire at about 1.9 kV with a diameter of 40 μm There are two cathode rings at both ends of the wires. The detector is filled with Helium and 4% ethanol for quenching. The coordinate perpendicular to the wire is obtained from the drift time, the coordinate along the wire from the time the Geiger discharge takes to propagate along the wire to the cathode pickup rings at each end. A 25G magnetic field is used to separate electrons from positrons.

Although some of the NEMO-III experience can be applied to the Super-NEMO design of a tracking detector, there are several new questions which need to be addressed before a prototype detector can be built. The first part is related to reducing the amount of material in the wire chambers to decrease absorption and energy loss of electrons through multiple scattering and to the general performance of the wire chamber. The second important aspect are the geometry and lay-out of the detector. Finally, methods and tools need to be developed to build a detector an order of magnitude larger than NEMO-III.

This sub-system is to be coordinated by the UK groups.

9.2.1 Prototype Cells

The aim of this work package is to build cell prototypes in order to demonstrate, in conjunction with LAL Orsay, and with the simulation work, a detector design and to find operating parameters that will be the

input to an engineering prototype.

The goals are to

1. reduce material and hence multiple scattering
2. increase wire length

From previous NEMO operating experience the following points need to be addressed . They are to a large extent highly interrelated parameters, and the goal is to find a suitable set of trade offs.

1. Construct Frame

   The frame construction will be carried out by a collaboration of an MSSL engineer with technical effort at Manchester along with direction from the French Engineer, Jacques Forget. The Manchester group would assemble a test set-up consisting initially of 9 Geiger cell prototypes about 2 m long using existing NEMO-III parameters as a working baseline. The envelope of cell parameters would then be slowly extended, by rewiring cells with smaller diameter wire, varying gas mixtures, by increasing wire length and by changing other parameters.

2. Readout for test cells

   The readout for the test cells will be a VME based system and use off the shelf items.

3. Wire Diameter

   The average amount of material that an electron from $\beta\beta$ decay passes through can be reduced by decreasing the wire diameter from 50 microns down to 40 or even 30 microns. Previous work has shown that the propagation of the Geiger discharge down the wire is very sensitive to non-uniformities in the wire diameter - NEMO 3 requires $< 1\%$ tolerance. Increasing length again increases this sensitivity. Furthermore, there are expected to be mechanical issues with wire fixing and tension.

4. Wire Material

   Alternatives to the currently used stainless steel need to be investigated, mainly for the cathode wires. Copper plated nylon has been tried unsuccessfully . LAL Orsay are interested in the idea of carbon fibre that has had its surface properties modified by ion implantation. Possible alternative wires are limited by radio purity considerations .

5. Wire Length

   The current wire length in NEMO-III is 2.7 m. Increasing the wire length improves the volume to surface ratio of the detector for no increase in channel count. A possible design goal is 4 m long wires. Geiger propagation in wires of this length needs to be tested as well as mechanical stability and gravitational effects on the wire.

6. Gas Composition

   Multiple scattering dictates Helium, with currently 1% Argon and 4% ethanol as quenchers to control the Geiger discharge. Changes to wire diameter and gas gain will require optimisation here.Although the experiment is intrinsically low rate, high gas gains over years have the potential for ageing. Additives such as ppm of water, reducing local surface fields, may have a role here. A clean gas system is required

7. 100 cell prototype

   After this R&D has been carried out and in light of the various trade-offs the Manchester group would take part of the responsibility of building and running a larger prototype of about 100 Geiger cells (at present envisaged as 4 m cells with 30 micron wire) to give better statistics on cell behaviour.

9.2.2 Tracker Readout Electronics

The Super-NEMO tracker consists of over 6000 drift cells operating in Geiger mode. Prompt signals from the wires give the perpendicular coordinate and and delayed signals from the Geiger rings give the position along the wire, so that the readout requires more than 12000 TDC channels operating with a number of thresholds and giving better than 20nsec resolution. This will be realised with an custom discriminator chip at or close to the detector feeding custom receiver boards that interface to the trigger and commercially sourced readout farm.

1. Tracker front end ASIC

   A collection of Application Specific Integrated Circuits (ASICs) were previously used in NEMO-III to implement the tracking readout. For Super-NEMO these ASICs will be combined and extended to provide the complete digitisation process at or very near the detector. The chips will include amplifiers and discriminators operating with several programmable thresholds and associated zero suppression logic. Data from the ASICs will be collected over serial data links and clock/trigger/control data will be fed to the ASICS over a serial link, minimising the number of connections to the detector. Some data reduction (zero suppression) and data storage (primary pipeline and event buffer) can be included, the exact specification of which depends on the requirements of the trigger system and the overall limits of ASIC complexity. For example, main data could be stored on the ASIC for asynchronous readout and data subset could be output promptly for use in forming the trigger. MSSL engineers will design and prototype this system.

2. Tracker Readout Boards

   To receive data transmitted from the front end ASICs, and to provide the uplinks providing the reference clocks and timing together with overall control of the ASIC we will develop custom readout boards. Concentrator boards will collect together data from a reasonable number (tens) of ASICs, providing further data reduction and producing trigger data in the required format. These boards might also perform first stage track segment reconstruction. Behind these the interface boards would feed data to the downstream DAQ farm over an industry standard interface (eg. USB2, Ethernet etc.). Second stage track reconstruction for triggering and online monitoring could be performed here. These boards will be designed and prototypes built by engineers at Manchester. For prototyping, some functions of the ASIC may be modelled using FPGAs

3. Active Foils

   One of the main backgrounds which need to be addressed in this proposed experiment is the decay of ^{214}Bi in the foil with subsequent β emission followed by a gamma which undergoes Compton scattering. The ^{214}Bi decay chain gives rise to 8 MeV alphas from the daughter ^{210}Po with a 164μ sec half life. Such heavily ionising particles have a maximum range of only 30cm in Helium but can be tagged to reject the events with some efficiency.

4. Prototype

   An active foil design is under consideration which consists of two thinner foils (15 mg/cm^2 instead of 50 mg/cm^2) with an active tracking volume in between. The idea is that thinner foils would increase the alpha tagging efficiency.

   Previous work focused on using short delayed tracks as an indirect signature of such an event. A possible alternative might be to directly detect the αs by running the central drift cells in semi-proportional mode. Issues to be addressed would be

   - is stable semi-proportional operation compatible with the gas mixture chosen for Geiger operation
   - Electrical pickup problems from adjacent Geiger cells firing
   - Is there an economical readout solution?

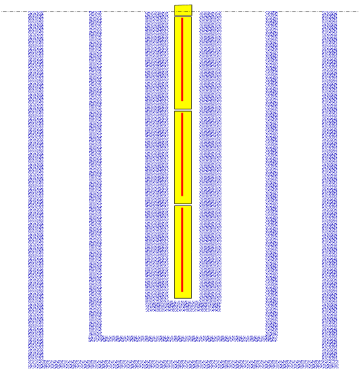

Figure 11: Example of planar geometry lay-out, The foil in the middle is completely surrounded by three layers where the inner layer has three and the outer two layers of Geiger drift tubes.

9.2.3 Wiring Robot

The Super-NEMO tracking detector will require between 20,000 and 50,000 drift cells with 9 wires each depending on the final design and detector lay-out. This large number of wires cannot be strung manually and a wiring robot needs to be constructed. In addition, the termination and crimping of the wires needs to be automated.

The cylindrical copper pick-ups at each end causes problems for a simple winding machine. A robot must be designed which is able to thread the wires through the copper pick-ups. An additional complication is due to the radiation requirements which exclude the use of solder.

Similar automated stringing systems are already in use in particle physics, for example in the BaBar experiment which used wiring robots and a control system from Adept Technologies, Inc.

1. Design

   A crimping system needs to be designed, based on the system currently used in NEMO, which is both efficient and cost effective. Cost effectiveness is an issue for Super-NEMO due to the large number of wires. For the option of using carbon fibres special crimping tools might have to be constructed.

   The design of the wiring robot is highly correlated with the geometric lay-out of the detector. In the first stage threading and crimping tools need to be developed.

2. Prototyping

   A small, table top, prototype will be built which will test the functionality of the threading and crimping tools.

9.2.4 Final Modifications

In this second stage, the exact specifications must be modified to the final chamber design to produce a full design specification ready to be produced as soon as the project is approved. This will be a critical path item for the Super-NEMO construction, and so it is vital that this is thoroughly specified by the end of this design study.

9.3 Calorimeter : R.Saakyan/F.Piqumel

Input:

Results from ongoing scintillator R&D, simulation results.

Output:

Optimum calorimeter layout with choice of block size and PMT type.

Milestones

- Optimisation of the thickness and composition of the scintillator for the calorimeter and design of the gamma catcher if necessary: Sep 05

Justification of Manpower

The series of measurements to be made are very time consuming and the manpower needed here is for the UCL RA to work together with Saakyan together with some tehcnical help (UCL tech) to make changes to the setup and analyse the data which will be taken.

To reach the planned sensitivity the Super-NEMO calorimeter will need energy resolution which is significantly better than that of the NEMO-III calorimeter ($FWHM = 15 - 17\%$ at $1MeV$). In order to achieve this goal an R&D programme was started in UCL a year ago with funds from the PPRP. This programme has demonstrated that a resolution of $8 - 9\%$ (FWHM) is achievable with a number of scintillator types using thinner blocks than NEMO-III and a status report is attached at Annex A. The target sensitivity for Super-NEMO can be reached if a background of $< 1 - 2$ events over the $500kg \times yr$ exposure (5 yr of data taking with 100 kg of ^{82}Se) can be achieved. The ultimate energy resolution needed for this will depend on the thickness of the source foil which is another item of this design proposal study, but initial calculations and MC showed that with 8-10% one could reach this background level.

Good calorimeter energy resolution has to be combined with reasonably good timing resolution. The timing resolution of the NEMO-III calorimeter is 250 ps (σ) which for Super-NEMO can probably be relaxed to 500 ps. Although achieving such a resolution does not represent a difficulty *per se* it is quite challenging when combined with a high energy resolution requirement.

9.3.1 Scintillator and PMT R&D programme : R.Saakyan

As a result of previous R&D programme described in Annex A, PVT has been identified as the baseline scintillator because it was demonstrated to have the target energy resolution for low energy electrons. There is still a number of items to be investigated to finalise the calorimeter design however and the main steps of this proposed R&D programme are summarised below. The majority of this scintillator R&D activity will be focused on PVT while the PST option is being pursued by French/Russian collaborators.

The Calorimeter sub-system is to be coordinated by the French groups.

1. Block Size Due to the large size of the Super-NEMO detector the minimum surface area of a single scintillator block should be probably not less than 20×20 cm^2 to keep the number of PMTs at a reasonable level. The surface covered by the scintillator calorimeter to accommodate 100 kg of ^{82}Se is ~ 400 m^2. Therefore 10000 PMTs will be needed if 20×20 cm blocks are used but $\sim$ only 4500 PMTs if 30×30 cm blocks are to be used. Simulations have to be carried out in order to find the optimum size of the scintillator block which should be a trade off between the number of PMT channels, detection efficiency and background tagging efficiency.

2. Uniformity of PVT Study the uniformity of light collection for a 20-30 cm single PVT block. Understand if the same resolution can be reached with such a block

3. Mosaic Scintillator Blocks It is not unlikely that with a large block the scintillator resolution will be worse. If this is the case a "mosaic" arrangement of several smaller optically isolated scintillators

viewed by the same PMT should be explored. Since a 7.5-8% resolution has been demonstrated with 9 cm blocks this possibility sounds promising but will have to be demonstrated.

4. Thickness Currently 2cm but if increase to 3-4 cm the probability of γ-detection can be increased to 20-30% which is essential for background rejection. Study the effect of the light guide on the resolution and its optimisation.

5. Scintillator Bars In this design instead of scintillator blocks long (from 1 to 2 m) scintillator bars with a cross-section of 10×2 cm^2 read out from both ends by two PMTs will be used. Such a layout will have clear advantages: just over 2000 PMTs will be needed; relatively cheap 5" flat window PMTs can be used eliminating the need for light guides; One scintillator wall is shared between two source foils reducing significantly the amount of scintillator needed; the detector becomes much more compact, one could accommodate 100 kg of the source in a setup occupying 10×10 m^2 floor space. These obvious advantages can only be exploited if an energy resolution comparable with that obtained from PMT-scintillator block assembly can be achieved. Preliminary estimates show that in this configuration the energy resolution requirement can be relaxed to $\sim$ 10% since thinner source foils can be used. However even 10% can be challenging for a scintillator detectors based on fairly long strips. We will conduct simulations of the light propagation inside the scintillator. The simulations will be followed by a small prototype aimed at demonstrating the feasibility of the method. For scintillator bar based technology the timing resolution should be also checked. We believe that this represents a very interesting opportunity and if vnecessary resolution is demonstrated and this layout option is chosen it will significantly affect the mechanical aspect of the design which will have to be done with close collaboration with our French colleagues.

6. Phoswich A possibility to combine a good energy resolution of a conventional widely available mineral scintillator with good timing resolution of plastic scintillator will be explored by studying the feasibility of using so called 'Phoswich' scintillators. The detector has two optically coupled layers: 3-4 mm of $CaF_2(Eu)$ and 1mm of a plastic scintillator. $CaF_2(Eu)$ has a large light output (25000 photons/MeV) and hence reaching a resolution of 5-6% at 1 MeV should be possible. A thin plastic scintillator will provide the necessary time resolution. Among other mineral scintillators $CaF_2(Eu)$ has an additional advantage of being a relatively low Z material which reduces the backscattering ratio for electrons.

7. PMT Studies This will include testing 5",8",10" and possibly 11" tubes from ETL and Hamamatsu. The characterisation of Photonis PMTs will be carried out by a group in Bordeaux. (A complimentary R&D programme in France and Russia is discussed below).

9.4 Trigger-DAQ : S.Kolya

Input

Input from NEMO-III on expected rates, and from design studies from the Scintillator, Calorimeter and Simulation workpackages.

Output

Prototype readout system and a design for a trigger/DAQ system for the TDR.

Justification of Manpower

The design and construction of a prototype trigger and DAQ system will mainly be performed by Scott Kolya.

The readout system for Super-NEMO has to reliably collect data from many channels at a low rate, but with a low dead time latency and with high availability. The only challenges presented by the readout are associated with the large channel count and the need to minimise radioactivity at or near the detector. This sub-system will be coordinated by the UK groups.

9.4.1 Clock and Control

Overall clock management and control of Super-NEMO is relatively straightforward when compared to a Particle Physics experiment with a large collection of sub detectors spread over a wide area. Within the scintillator and tracking readout overall synchronisation and control is handled by the underlying design. Some additional work may be required to tie together the tracking, scintillator and trigger subsystems, and to interface this to overall run control, and any additional hardware required for this could be designed at Manchester. This may include a global timing reference.

9.4.2 PC Farm for Data Acquisition

Data collection for analysis will be performed by a small farm of PCs logging data to RAID disk arrays. This is a Commercial-Off-The-Shelf (COTS) system based on commodity computing products as available at the time. Neither the data rate or the anticipated processing present any challenges to today's PCs. Interface to the custom electronics will be via an industry standard interface to allow for easy upgrades as required. The system would run a commercial real time operating system or real time Linux.

Manchester will research the specification of this system but we do not foresee the need to prototype a full system at this stage. Any standalone readout systems used for the testing of prototypes will, wherever possible, follow these specifications so as to ease the subsequent transition to the full detector system.

9.5 Light Injection Calibration System : J.Thomas

Input

Experience from MINOS light injection system, and from NEMO-III prototype LED calibration system.

Output

Prototype system to be used to track gains and linearity of PMTs.

Justification of Manpower

This will be essentially carried out by Thomas with 10% of the UCL RA's time for data analysis and validation of the calibration accuracy.

A light injection calibration system is required to monitor, and to compensate for, changes in amplification (and non-linearity) of the photo tubes. We are expecting to draw heavily on the previous design experience at UCL of the MINOS light-injection calibration system which is now being used to calibrate 20,000 PMT channels. Ultra bright blue, or UV LEDs are cheaply available commercially and are bright enough to be fanned out to many PMTs via optical fibre. Tests of this concept, using the LED-fibre coupling 'cone', designed at UCL for MINOS have already commenced and will be expanded to tests at NEMO-III in the near future.

This subsystem will be coordinated by UCL.

9.5.1 Pulser

A dedicated pulser will probably have to be designed to drive the LEDs for reasons of cost. In this case the design can be taken directly (with some minor modifications) from the MINOS pulser box design developed at Sussex. However it is possible that a commercially available pulse generator could be used if the LEDs are bright enough such that only one or two are needed for the entire system.

9.5.2 Light distribution system

There is a number of issues which will have to be investigated.

- Blue LEDs versus UV LEDs
- The injection of light directly into PMT or via scintillator
- The maximum number of PMT channels which can be illuminated by a single LED. Realistic (long) lengths of optical fibres will have to be used.
- Possible artificial non-linear effects due to the small variations in wavelength emitted by the LEDs will be studied.

The performance of the LED based light-injection system will be initially studied using the setup dedicated to the scintillator R&D which with some modifications can include up to 10-20 PMT channels.

9.6 Technical Design Report : J.Thomas/C.Auger

Input

Results from all workpackages.

Output

TDR documenting the full design of the Super-NEMO module, the building block of Super-NEMO.

Justification of Manpower

Everyone involved will be contributing to this effort. This is the culmination of all the previous effort and so the amount of manpower needed here should not be underestimated.

Goal

Production of a full technical design of the Super-NEMO module.

The TDR will be written on the outcome of the R&D outlined here. It is expected that there will be some final simulations and optimisation to be done during this time so a fair amount of time and manpower has been allocated to this task.

9.7 Source Foils

The production of the foil will be carried out in Russia. It is a relatively straightforward and well practised procedure and has been practised numerous times before for NEMO-III. If the order can be placed well in advance, there is no reason why this component should present any problems.

This sub-system will be coordinated by the French groups in collaboration with ITEP.

9.8 Material Purity Measurement

For all materials which will be used to build the Super-NEMO detector, there will need to be an assessment of the purity with respect to ^{238}U and ^{232}Th background. This evenutally will be a major task when building Super-NEMO because every piece will need to be measured. For this design study, it is expected that the material samples which are used for the frame, wires, scintillator and PMTs will need to be assessed, and we are hoping that we will be able to make use of the Boulby Low Background Counting Facility currently

at the stage of proposal writing. If this facility is not approved inthe next year, then our measurements will have to be carried out at Modane. In this case, for the final Super-NEMO project, we would be expected to contribute some number of Germanium detectors for this effort.

This sub-system will be coordinated by the French groups.

10 Industrial Involvement

Strong links with industry have already been formed with Hamamatsu(Japan) and ETL(UK) from whom we will purchase the PMT samples for testing. The results from the measurements will be fed back to the companies. Eventually, this R&D will lead to a very large order of PMTS worth several millions of pounds if the project is funded. Also, ties have been developed between UCL and Photonic Materials(UK), a company who make fast mineral scintillator and development of this 'magic' crystal is the subject of a bid to the PPARC Innovative Technology fund.

11 Risks

The Super-NEMO proposal is based on a reasonable extension of existing technology and many of the underlying technological and physical principles have been proved to work in the current NEMO-III experiment. The main challenges are related to the improvement of the performance of the detector, such as calorimeter energy resolution and the increased wire lengths for the tracking chambers. Another challenge is the scaling of the construction by an order of magnitude compared to NEMO-III.

Risks which would delay construction of the detector or increase construction times are small because there is no external schedule to match as in the case of an accelerator based experiment. In such a case the experiment could be constructed in steps due to the modular design and data could be taken with a smaller detector while the full detector is constructed. Table 2 outlines the specific risks.

12 Manpower and Resources

A new facility at MSSL will be at the disposal of the UCL/HEP group for the R&D work outlined here and for the eventual construction of several of the Super-NEMO modules if the project is approved. This will vastly improve the hardware capabilities of the UCL group and it is natural that the very extensive technical capability of the MSSL group will be made use of wherever possible paving the way for a new symbiotic relationship between HEP and Space Science. UCL have personnel who have been extensively involved in building calorimeters(MINOS),TPCs(ALEPH),PMT Development(MINOS), IPCs(GEM),Light injection calibration systems (MINOS,NEMO-III) as well as very low background physics experiments (NEMO-III,DBA). At UCL there is previous experience in running the wiring and crimping robot for the ZEUS Central Tracking Detector (24,000 wires).

The Manchester group has extensive lab space for construction as well as expertise in tracking chamber construction which is being made use of. UCL and Manchester have considerable DAQ and electronics expertise. The Manchester group had a central role in building the muon chambers for the JADE experiment at DESY and the OPAL experiment at CERN . Ray Thompson was responsible for the assembly of the Muon chambers of H1 which consists of 1800 drift cells. He also worked on the inner tracker planar chambers of the H1 experiment and the Manchester group performed studies for Gas Microstrip detectors during the early stages of ATLAS.

The Manchester TDAQ group had responsibility for the tracking readout at H1, and participated in the H1 FTT trigger upgrade (including design of the clock/control and associated hardware). They have recently

Risk	Effect	Likelihood	Impact	LxI	Mitigation
Tracker Work Package					
Cannot extend working envelope to 4m wire length	Redesign of tracker geometry and simulation	2	1	2	flexible geometry definition
Wiring/Crimping cannot be fully automated	longer construction/ higher cost	1	2	2	smaller detector allow for extra costs
Calorimeter work package					
Energy resolution can not be achieved in large blocks	smaller blocks will add to cost	1 1	2 2	2 2	Mosaic arrangement possible to keep blocks small
Overall Project					
Radiopurity level of source foils cannot be reached	sensitivity can drop by factor of up to 2	1 1	2 2	2 2	2nd cycle of purification necessary
No location suitable	affects design and costs	2	2	4	Buy underground volume
Low Background facility not approved	material activity measurements more difficult	2	1	2	Plan for French labs (Modane)

Table 2: Table showing specific risks

delivered an FPGA based track segment finder to BaBar as part of a L1 trigger upgrade. These boards were designed and built by the Manchester group.

Institution	Category	Name	Manpower 05	Manpower 06
UCL	T	Gianfranco Sciacca	40%	40%
UCL	E	Janet Fraser	10%	20%
UCL	E	Brian Anderson	20%	30%
UCL	E	Gordon Crone	0%	10%
MANCHESTER	T	Julian Freestone	10%	10%
MANCHESTER	E	Scott Kolya	10%	30%
MANCHESTER	P	Steve Snow	0%	10%
MANCHESTER	E	Ray Thompson	10%	10%
MANCHESTER	T	Andrew Elvin	10%	10%

Table 3: Table showing rolling grant effort

Institution	Category	Name	Manpower 05	Manpower 06	Total Cost
UCL	P	New Post	100%	100%	100k
UCL/MSSL	E		100%	100%	140k
UCL/MSSL	T		80%	80%	84k
MANCHESTER	P	New Post	100%	100%	100k
total					424k

Table 4: Table showing requested extra effort

13 International Collaboration

Some work on the prototyping of a Super-NEMO module has already been carried out by the Orsay engineering group. A meeting to exchange information between the Orsay and UK engineers (from MSSL and Manchester) has already taken place. A meeting between the French and UK collaborators to agree on the separation of the work packages took place in mid-January and the French groups submitted their proposal to their funding agency in late March which has been met very positively. They are awaiting the result of this submission to PPARC, because without UK funding, it is probable that the French agency will reduce the rate at which money is awarded. It is clear that without the UK, there is no obvious path to completing the detector after the design study.

The French are predominantly to be involved in the calorimeter design, as well as trigger and some tracking prototyping. They have extensive expertise in all aspects of this type of experiment.

At the Super-NEMO collaboration meeting in early April 2005, the Super-NEMO Steering Committee was formed comprising one representative of each institute. This will represent the main collaboration structure defining body through out the timespan of this design study. It is expected that other structures will be put into action as time goes on and as the work load requires. At the meeting in April, the overall responsibilities for the main work packages were assigned and are reported in the programme of work in Section 9.

14 Travel

We expect that there will be a significant amount of travel associated with the international and national collaboration. Table 6 shows an estimated break down of the costs.

Institution	Category	Manpower 05	Manpower 06
UCL	Physicist	100%	100%
UCL	Academic	80%	80%
UCL	Academic	40%	40%
UCL	Engineer	30%	60%
UCL	Technician	40%	40%
UCL/MSSL	Engineer	100%	100%
UCL/MSSL	Technician	80%	80%
MANCHESTER	Physicist	100%	110%
MANCHESTER	Academic	25%	25%
MANCHESTER	Academic	10%	10%
MANCHESTER	Engineer	20%	40%
MANCHESTER	Technician	20%	20%

Table 5: Table showing total effort including academic effort and requested extra effort

Description	Cost per trip £	No of person-trips in 2 years	Total Cost £
UK travel	£200	200	40k
International Travel	£400	100	40k
Total			80k

Table 6: Table showing estimated costs for travel

Figure 12: Gant chart for the plan of work.

15 Table Summary

15.1 Costs of Workpackages

15.1.1 Workpackage 1 : Simulation

1.0 Simulation	2005	2006
UCL Academic	20%	
Manchester Academic	20%	10%
UCL RA (30%,0)	£15,000	
Manchester RA (50%,0)	£25,000	
Total	£40,000	

Table 7: Table showing estimated costs for simulation staff

1.0 Simulation	Item	Cost 05
Staff		£40,000
Equipment		
Consumables		
Travel		£4,000
Exceptional		
Total		£44,000

Table 8: Table showing estimated total costs for simulation

15.1.2 Workpackage 2 : Tracker

Description	Cost £
Lecroy waverunner oscilloscope	13k
CAEN HV Mainframe	7.5k
HV modules(4)	7.2k
VME interface for HV system	1.8k
NIM Discriminators	4.4k
NIM Coincidence Logic	1.5k
VME FADC cards x2	8.4k
PC	2.2k
Test tank + feedthroughs	2.5k
Tension Measuring device	1.5k
Wire,crimps,pickup rings	3.0k
Brooks electronic flow meters + controller	4.8k
Oxygen meter	3.2k
Gas	0.5k
Radioactive Sources	1.5k
100 cell prototype components	10k
Gas System (stainless steel pipe, fitting,filters,mixer,chiller)	3k
Solder paste,nozzles,other consumables	1k
Robot Components	
Steel and Aluminium Alloy stick sections	20k
Bearings, springs, lubrication fittings, fixings	5K
Motors and servo accessories	20K
Pneumatic system components	5K
Total	127k

Table 9: Table showing estimated costs for tracker development

2.0 Tracker	2005	2006
UCL Academic	50%	50%
Manchester Academic	15%	25%
UCL RA (40%,70%)	£20,000	£35,000
Manchester RA(50%,50%)	£25,000	£25,000
Manchester RG/P (0,10%)		£5,000
UCL eng (30%,60%)	£21,000	£42,000
MSSL Tech (80%, 80%)	£42,000	£42,000
MSSL Eng (100%,100%)	£70,000	£70,000
Manchester Eng (20%,20%)	£14,000	£14,000
Manchester Tech(20%,0%)	£10,000	
Total	£202,000	£233,000

Table 10: Table showing estimated costs for tracker development staff

2.0 Tracker	Item	Cost £
Staff		£435,000
Equipment	See Table 9	£73,600
Consumables	See Table 9	£53,000
Travel		£48,000
Exceptional		
Total		£610,000

Table 11: Table showing estimated total costs for tracker development

15.1.3 Workpackage 3 : Calorimeter

Description	Cost £
Plastic Scintillator PVT BC404,BC408 blocks	2k
Plastic Scintillator PVT BC404,BC408 bars	2k
Plastic Scintillator PVT BC404,BC408 blocks and strips	1k
Mineral Scintillator CaF2(Eu)	3k
Mineral Scintillator YSO/YAP	3k
Hamamatsu low bgd PMTs, 5,8 and 10 inches	5k
ETL low background, 5,8,11 inches	5k
ETL glass free	5k
VME crate and controller	6k
VME ADC and FADC 0.1-1Ghz	5k
VME custom built trigger logic board	3k
3 x Calibration source Bi207	3k
electron spectrometer with Sr90 source	4k
Total	47k

Table 12: Table showing estimated cost of Calorimeter R&D

3.0 Calorimeter	2005	2006
UCL Academic	50%	40%
UCL RA (30%,10%)	£15,000	£5,000
UCL Tech (40%,30%)	£26,000	£21,000
Total	£41,000	£26,000

Table 13: Table showing estimated cost of Calorimeter R&D Staff

3.0 Calorimeter	Item	Cost £
Staff		£67,000
Equipment	See Table 12	
Consumables	See Table 12	£47,000
Travel		£12,000
Exceptional		
Total		£124,000

Table 14: Table showing estimated total cost of Calorimeter R&D

15.1.4 Workpackage 4 : Trigger DAQ

Description	Cost £
Prototype concentrator (x4)	12k
Prototype Receiver (x4)	12k
Custom Crate	6k
PC systems for prototype (x2)	4k
Development of embedded FPGA readout for prototype	3k
Total	37k

Table 15: Table showing estimated costs for Trigger-DAQ development

4.0 Trigger/DAQ	2005	2006
Manchester Eng(0,20%)		£14,000
Manchester RA (0,40%)		£20,000
Manchester Tech (0,20%)		£10,000
Total		£44,000

Table 16: Table showing estimated costs for Trigger-DAQ Staff

4.0 Trigger-DAQ	Item	Cost
Staff		£44,000
Equipment	See Table 15	£10,000
Consumables	See Table 15	£27,000
Travel		£12,000
Exceptional		
Total		£93,000

Table 17: Table showing estimated total costs for Trigger-DAQ

15.1.5 Workpackage 5 : Light Injection

Description	Cost £
LEDs, materials	2k
Pulse Generator	5k
Optical Fibres	3k
Total	10k

Table 18: Table showing estimated costs for light inection calibration system development

5.0 Light Injection	2005	2006
UCL Academic		20%
UCL RA (0,10%)		£5,000
UCL Tech (0,10%)		£7,000
Total		£12,000

Table 19: Table showing estimated costs for Light Injection Staff

5.0 Light Injection	Item	Cost
Staff		£12,000
Equipment	See Table 18	£5,000
Consumables	See Table 18	£5,000
Travel		£4,000
Exceptional		
Total		£26,000

Table 20: Table showing estimated total costs for Light Injection

15.1.6 Workpackage 6 : Technical Design Report

5.0 Light Injection	2005	2006
UCL Academic		10%
UCL RA (0,10%)		£5,000
Manchester RA (0,10%)		£5,000
Total		£10,000

Table 21: Table showing estimated costs for TDR Staff

6.0 Technical Design Report	Item	Cost
Staff		£10,000
Equipment		
Consumables		
Travel		
Exceptional		
Total		£10,000

Table 22: Table showing estimated total costs for TDR

15.2 Staff Effort Overview per Institute

UCL Staff	2005/06	2006/07
New RA	£50,000	£50,000
Technicial	£26,000	£28,000
Engineer	£21,000	£42,000

UCL/MSSL Staff	2005/06	2006/07
Technicial	£42,000	£42,000
Engineer	£70,000	£70,000

Manchester Staff	2005/06	2006/07
New RA	£50,000	£50,000
RG Physicist	£	£5,000
Engineer	£14,000	£28,000
Technician	£10,000	£10,000

15.3 Overview of costs to PPARC

	2005/06	2006/07	total
Staff Effort			
UCL	£97,000	£120,000	£217,000
Manchester	£74,000	£93,000	£167,000
UCL/MSSL	£112,000	£112,000	£224,000
Equipment			
Simulation			
Tracker	£63,500	£63,500	£127,000
Calorimeter	£23,500	£23,500	£47,000
Trigger-DAQ	£18,500	£18,500	£37,000
Light Injection	£5,000	£5,000	£10,000
Travel			
Simulation	£2,000	£2,000	£4,000
Tracker	£24,000	£24,000	£48,000
Calorimeter	£6,000	£6,000	£12,000
Trigger-DAQ	£6,000	£6,000	£12,000
Light Injection	£2,000	£2,000	£4,000
Total	£433,500	£475,500	£909,000

16 Contingency

We believe the main uncertainty throughout this proposal is the amount of manpower needed. Microsoft project has been used to estimate total manpower but unforeseen technical difficulties can often occur. We would recommend a 50% contingency on manpower. In addition, if the Boulby Low Background facility does not go ahead in the near future, we would have to make a further request to PPRP at a later date for £150k for a 1 litre HPGe detector to be located in the Modane Underground Laboratory.

17 The Request

We are requesting new money of £725k over the two year period, and £184k of already funded rolling grant effort. We summarise the Super-NEMO Design Study project costs in Table 23 from the subsystem costs as outlined in Tables 2-5.

18 Conclusion

This proposal represents the work needed to turn the ideas of the Super-NEMO collaboration into a fully designed experiment which could then be built within a time frame of about three years following approval. In this case, Super-NEMO will reach a sensitivity of ~ 0.04eV by 2014. On this time scale, Super-NEMO would be competitive with the forefront experiments being planned around the world. The unique feature of Super-NEMO is its cabability to measure almost any isotope by identifying a clear topological and energetic signature of the $0\nu\beta\beta$ decay and these features will propel it into the position of the most important next generation double beta decay experiement in the coming decade.

Description	Cost £
Calorimeter R&D	47k
Tracker	77k
Wiring Machine	50k
Light Injection	10k
Trigger-DAQ hardware	37k
Manpower RAs	200k
Manpower Engineer, Technical	224k
Travel	80K
Total	725k

Table 23: Table showing total new money request

Appendix Scintillator R&D Status Report

18.1 Executive Summary

A year ago, the PPRP awarded Saakyan and Thomas funds to carry out a short programme of R&D aimed at reaching an energy resolution in the Super-NEMO calorimeter blocks of better than 10%, necessary to deliver Super-NEMO a background free measurement of the $0\nu\beta\beta$ in the case it is in the reach of this proposed experiment. Shortly therafter, Manchester joined the effort, focussing on simulation of the $0\nu\beta\beta$ electrons in various scintillators. The status of this work is reported below.

18.2 Introduction

The motivation to improve the energy resolution from the 15% exhibited in NEMO-III to better than 10% is laid out in Section 6.2.

This programme of R&D has demonstrated that a resolution of 8% (FWHM) is achievable with a number of scintillator types. The status of the R&D measurements and results is presented here. Although this report does not represent the final results from this R&D programme, it represents a snapshot of the (substantial) progress to date.

18.3 Scintillator Measurements

The scintillator R&D at UCL has been focussed on studying the effect of various scintillator parameters on its light output when electrons and gammas are incident on it. In doing so, the light collection efficiency from the plastic (organic) scintillator has been improved. Instead of polystyrene used in NEMO-III a different plastic scintillator has been studied, namely polyvinyltoluene (PVT) which, according to the manufacturer's (Bicron) specifications, should have a higher light output. The two most promising samples in terms of light output were BC-404 and BC-408. We have studied samples of three different sizes: 2cm $\times$ 2cm $\times$ 2cm, 5cm $\times$ 5cm $\times$ 2cm, 9cm $\times$ 9cm $\times$ 2cm. The 2 cm thickness was chosen to optimise the energy resolution of the detector to electrons in the MeV region while still maintaining a reasonable ($\sim$ 15%) efficiency of photon detection which is essential for background rejection in a NEMO like detector.

A sketch of the setup used for the measurements is shown in Figure 13.

A ^{207}Bi conversion electron source has been used for the measurements. This source has two peaks from conversion electrons: a strong peak at 976 KeV (K-line) and a weaker peak at 482 KeV (K-line) as well as two gamma lines at 1064 KeV and 570 KeV which in plastic scintillator are seen only via Compton scattering. In order to obtain "pure" electron events in the scintillator a background subtraction is carried

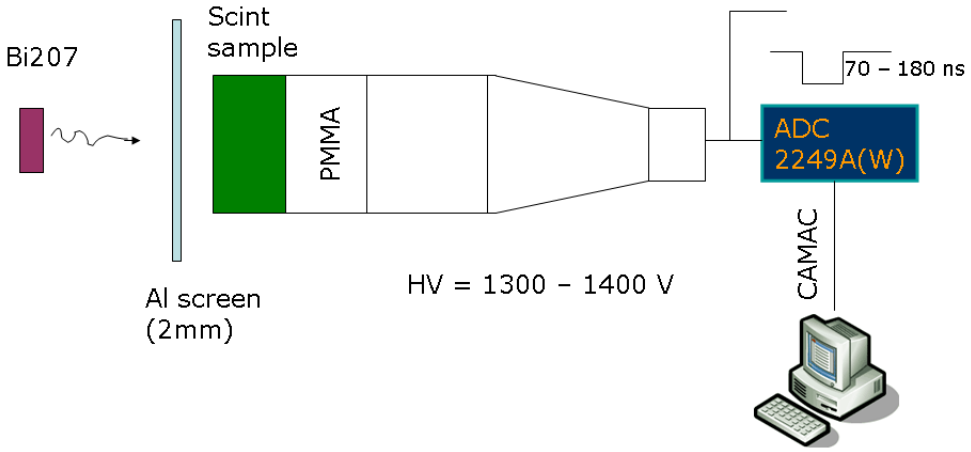

Figure 13: A highly schematic view of the setup used for the scintillator R&D.

out. The data is taken with and without a 2mm thick aluminium filter placed between the source and the scintillator block. The spectra without the filter include both electron and gamma events while the spectra with the filter have only the γ component. Typical spectra are shown in Figure 14. The subtraction gives a conversion electron spectrum which is shown in Figure 15.

To calculate the energy resolution of the detector the 976 KeV peak was fitted with a sum of three gaussian functions with appropriate weights and central mean values corresponding to the relative intensities and energies of the K, L and M (976KeV, 1049KeV, 1061KeV) lines of the 1064 KeV transition. A typical result of the fit is shown in Figure 16.

The R&D programme so far has been focused on the following studies:

- Comparison between BC404 and BC408 samples of different sizes
- The effect of surface treatment on the light output (polished versus depolished surface
- Scintillator to PMT coupling: optical gels, measurements with and without light guides
- Scintillator coating material: mylar, teflon, tyvec
- PMT studies: finding an operation regime at which the secondary emission ration does not contribute significantly to the energy resolution
- Comparison between three PMTs: Hamamatsu 5" with hemispherical window, ETL 5" with flat window and ETL 8" with hemispherical window

The best resolution of ~7.5% (FWHM at 1 MeV) was obtained with the ETL flat window 5" PMT and BC404 scintillator with depolished surface and wrapped in a mixture of aluminized mylar and tyvec. The series of results are summarised in the Tables 24, 25 and 26. The presentation is in tabular form because there is no discernable difference in the spectra to the eye between 7 and 10%.

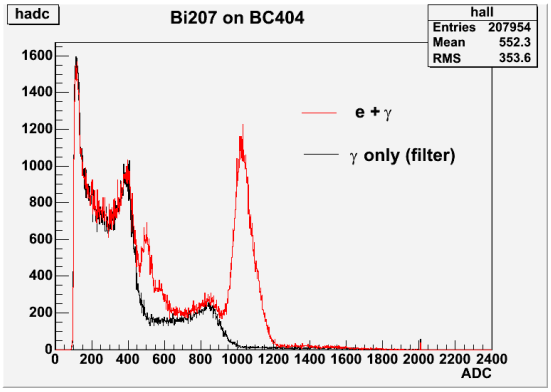

Figure 14: Typical ^{207}Bi spectra taken with BC-404 plastic scintillator with (red) and without (black) the Al-filter.

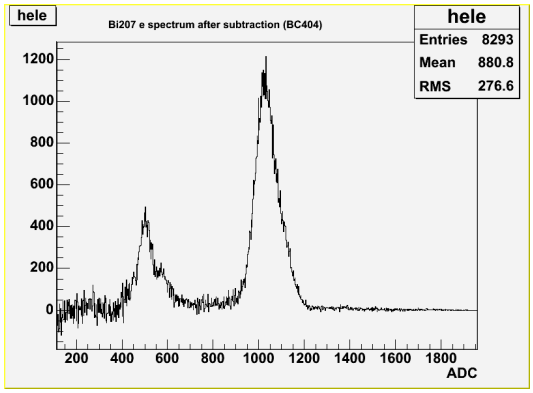

Figure 15: A ^{207}Bi conversion electron spectra obtained from the subtraction experiment (see text). 482 KeV and 976 KeV peaks are clearly seen.

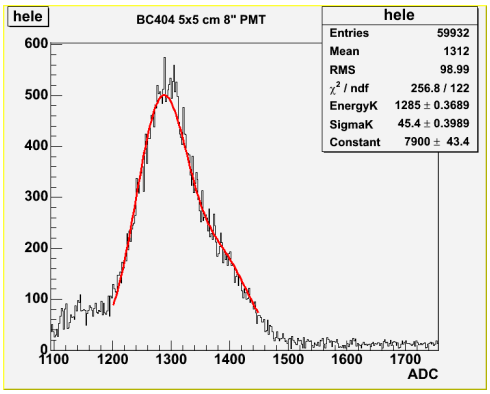

Figure 16: The 976 KeV conversion electron peak fitted with three gaussians corresponding to the K, L and M lines of the 1064 KeV transition of ^{207}Bi.

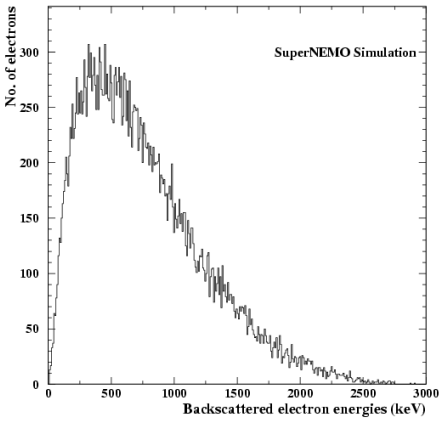

Figure 17: Energy distribution of electrons backscattered from a organic scintillator into the tracking volume using a GEANT-3 simulation of $0\nu\beta\beta$ decays.

18.4 Simulations

At this energy (order 1 MeV) some electrons are actually scattered back from the scintillator, the fraction depending on the atomic number (Z) of the material.

The amount of backscattering of electrons from the scintillator into the tracking volume is an important factor in determining the scintillator material. A possible increase in background and decrease in detection efficiency from backscattering must be weighed against the improvement in energy resolution which can be obtained using inorganic scintillator materials. The Manchester group has simulated this effect using a GEANT-3 simulation. Figure 17 shows the energy distribution of backscattered electrons for an organic scintillator material. The backscattering ratio, defined as the ratio of electrons from β decays leaving the volume over the number of electrons entering it, is approximately 20% for an organic scintillator in the GEANT-3 simulation and it increases to about 25% using pure Yttrium which is the main component in some of the inorganic scintillators tested. More detailed background studies in the future are needed to determine the influence of backscattering on background and detection efficiency.

18.4.1 Geometric Acceptance

The GEANT-3 simulation was used to perform preliminary studies of the geometric acceptance for the proposed Super-NEMO designs. In this simulation the tracking volume is completely surrounded by scintillators. The distance between the foil and the scintillators parallel to the foil is chosen to be 50 cm and the distance between the end of the foil and the scintillator section orthogonal to it is 10 cm. In Figure 18 the acceptance ratio, defined as the number of $0\nu\beta\beta$ events where both electrons are detected divided by all generated $0\nu\beta\beta$ events, is shown as a function of the coordinate of the decay vertex in the foil. An electron must have a length of 35 cm to be accepted, no detailed simulation using wire hits has been performed yet. The acceptance ratio drops from about 65% to about 30% at the edges of the foil. In the future a more detailed version of this simulation will be used to determine the geometric parameters of the chambers.

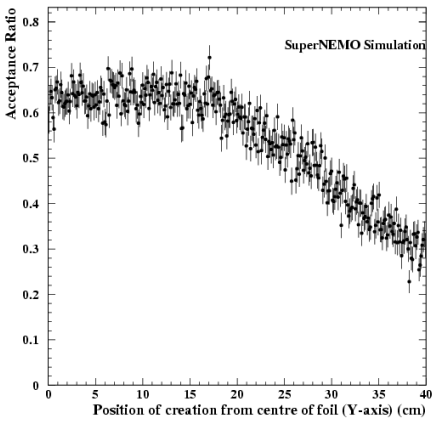

Figure 18: Acceptance ratio, defined as the number of $0\nu\beta\beta$ events where both electrons are detected divided by all generated $0\nu\beta\beta$ events, as a function of the coordinate of the decay vertex in the foil.

Table 24: FWHM Energy resolution for 1 MeV electrons obtained with the 5" ETL phototube (no light guide) and PVT scintillators of different sizes. Scintillator coating and surface treatment studies

Scintillator	Size, cm^3	Surface treatment	Coating	$\Delta E/E$, %
BC404	$2 \times 2 \times 2$	Standard	No	10.4
BC404	$2 \times 2 \times 2$	Polished	No	10.6
BC404	$2 \times 2 \times 2$	Depolished	No	10.3
BC404	$2 \times 2 \times 2$	Depolished	Mylar	8.2
BC404	$2 \times 2 \times 2$	Depolished	Tyvec	8.5
BC404	$2 \times 2 \times 2$	**Depolished**	**Tyvec/Mylar**	**7.9**
BC408	$2 \times 2 \times 2$	Standard	No	10.9
BC408	$2 \times 2 \times 2$	Polished	No	10.7
BC408	$2 \times 2 \times 2$	Depolished	No	10.5
BC408	$2 \times 2 \times 2$	Depolished	Mylar	8.6
BC408	$2 \times 2 \times 2$	Depolished	Tyvec	8.8
BC408	$2 \times 2 \times 2$	**Depolished**	**Tyvec/Mylar**	**8.0**
BC404	$5 \times 5 \times 2$	Standard	No	10.1
BC404	$5 \times 5 \times 2$	Polished	No	10.1
BC404	$5 \times 5 \times 2$	Depolished	No	9.4
BC404	$5 \times 5 \times 2$	Depolished	Mylar	7.8
BC404	$5 \times 5 \times 2$	Depolished	Tyvec	8.2
BC404	$5 \times 5 \times 2$	**Depolished**	**Tyvec/Mylar**	**7.4**
BC408	$5 \times 5 \times 2$	Standard	No	10.3
BC408	$5 \times 5 \times 2$	Polished	No	10.2
BC408	$5 \times 5 \times 2$	Depolished	No	9.7
BC408	$5 \times 5 \times 2$	Depolished	Mylar	8.2
BC408	$5 \times 5 \times 2$	Depolished	Tyvec	8.5
BC408	$5 \times 5 \times 2$	**Depolished**	**Tyvec/Mylar**	**7.7**
BC404	$9 \times 9 \times 2$	Standard	No	10.2
BC404	$9 \times 9 \times 2$	Polished	No	10.3
BC404	$9 \times 9 \times 2$	Depolished	No	9.2
BC404	$9 \times 9 \times 2$	Depolished	Mylar	7.9
BC404	$9 \times 9 \times 2$	Depolished	Tyvec	8.2
BC404	$9 \times 9 \times 2$	**Depolished**	**Tyvec/Mylar**	**7.5**
BC408	$9 \times 9 \times 2$	Standard	No	10.2
BC408	$9 \times 9 \times 2$	Polished	No	10.1
BC408	$9 \times 9 \times 2$	Depolished	No	9.5
BC408	$9 \times 9 \times 2$	Depolished	Mylar	8.0
BC408	$9 \times 9 \times 2$	Depolished	Tyvec	8.4
BC408	$9 \times 9 \times 2$	**Depolished**	**Tyvec/Mylar**	**7.9**

Table 25: FWHM Energy resolution for 1 MeV electrons obtained with BC404 $5 \times 5 \times 2$ cm^3 wrapped in Tyvec/Mylar. PMT and light guide studies

PMT	Light Guide	Light Guide coating	$\Delta E/E$, %
Hamamatsu R6594 5”	PMMA	No	12.0
Hamamatsu R6594 5”	PMMA	Mylar	9.0
ETL 9354 KB 8”	PMMA	No	11.5
ETL 9354 KB 8”	PMMA	Mylar	8.7
ETL 9354 KB 8”	PMMA	Tyvec	8.2
ETL 9354 KB 8”	**NO**	***	**7.8**
ETL 9390B 5” flat window	**NO**	***	**7.4**

Table 26: FWHM Energy resolution for 1 MeV electrons obtained with the 5” ETL phototube.

Scintillator type	Size, cm^3	$\Delta E/E$, %
BC404	$2 \times 2 \times 2$	7.9
BC408	$2 \times 2 \times 2$	8.0
BC404	$5 \times 5 \times 2$	7.4
BC408	$5 \times 5 \times 2$	7.7
BC404	$9 \times 9 \times 2$	7.5
BC408	$9 \times 2 \times 2$	7.9

18.5 Conclusion

A large amount of data now exists on scintillator geometry and optical coupling to PMTs of different types. An energy resolution of 7.5% has been achieved using the optimal choice of coupling, scintillator and PMT. However, many of the samples tested produce a resolution of 8% or better, below the 10% goal of the R&D proposal. The key to this success is in the use of thin scintillator (order few cm), with the down side of a loss in gamma efficiency. This can be regained using a separate gamma-catcher arrangement, so it is certainly not a show stopper. The chief outcome of this programme has been the demonstration of better than 10% resolution using organic (PVT) scintillator.

References

[1] Yanagida T., *Proc. Workshop on Unified Theory* Sawada and Sugamoto eds., KEK (1979);
Gell-Mann M., Ramond P. and Slansky R., *Supergravity* van Nieuwenhuizen and Freedman eds., North Holland, Amsterdam (1979).

[2] Heidelberg-Moscow collaboration, H.V. Klapdor-Kleingrothaus *et al.*, Eur. Phys. J. A 12, 147 (2001);
IGEX Collaboration, C.E. Aalseth *et al.*, Physics of Atomic Nuclei 63 (2000) 1225.

[3] E. Fiorini, Phys. Rep 307 (1998) 309;
H.V. Klapdor-Kleingrothaus *et al.*, J. Phys. G 24 (1998) 483;
C.E. Aalseth *et al.*, hep-ex/0201021;
M. Danilov *et al.*, Phys. Lett. B480 (2000) 12.

[4] A.Fauessler et al, Nucl-th/0503063
Bryan W. Lynn, Nucl.Phys.B402:281-322,1993 CHIRAL SU(2)-L X SU(2)-R LIQUIDS: A THEORY OF HEAVY NUCLEI AND NEUTRON STARS.

[5] J. Suhonen and O. Civitarese, Phys. Rep. 300, 123 (1998).

[6] L. De Braeckeleer et al., Phys. At. Nucl. 63, 1214 (2000).

[7] A. Barabash et al., to be submitted to Phys. Lett. B.

[8] S.Stoica et al.,Nucl. Phys. A694 (2001).

[9] P. Minkowski, Phys. Lett. B **67** (1977) 421;
M. Gell-Mann, P. Ramond and R. Slansky, in *Supergravity*, eds. D.Z. Freedman and P. van Nieuwenhuizen (North-Holland, Amsterdam, 1979);
T. Yanagida, in Proc. of the *Workshop on the Unified Theory and the Baryon Number in the Universe*, Tsukuba, Japan, 1979, eds. O. Sawada and A. Sugamoto;
R. N. Mohapatra and G. Senjanović, Phys. Rev. Lett. **44** (1980) 912.

[10] E. Witten, Nucl. Phys. B **268** (1986) 79;
R.N. Mohapatra and J.W.F. Valle, Phys. Rev. D **34** (1986) 1642.

[11] G. B. Gelmini and M. Roncadelli, Phys. Lett. B **99** (1981) 411.

[12] C. S. Aulakh and R. N. Mohapatra, Phys. Lett. B **119** (1982) 136.

[13] G. Bhattacharyya, H. V. Klapdor-Kleingrothaus, H. Paes and A. Pilaftsis, Phys. Rev. D **67** (2003) 113001.

[14] H. V. Klapdor-Kleingrothaus, H. Paes and U. Sarkar, Eur. Phys. J. A **5** (1999) 3.

[15] M. Fukugita and T. Yanagida, Phys. Lett. B **174** (1986) 45;
A. Pilaftsis and T.E.J. Underwood, Nucl. Phys. B **692** (2004) 303; hep-ph/0506107.